PHYSICAL REVIEW B VOLUME 50, NUMBER 9 1 SEPTEMBER 1994-I

Thermal conductivity of a-Si:H thin films

David G. Cahill, M. Katiyar, and J. R. Abelson
Department of Materials Science and Engineering, Materials Research Laboratory, and Coordinated Science Laboratory, University of Illinois, Urbana, Illinois 61801
(Received 18 February 1994)

The thermal conductivity of sputtered a-Si:H thin films for a hydrogen content of 1–20 % and a film thickness of 0.2–1.5 μm is determined in the temperature range 80–400 K using an extension of the 3ω measurement technique. The reliability of the method is demonstrated on 1-μm-thick a-SiO_2 thermally grown on Si. Scattering of phonons at the interface between the a-Si:H film and the substrate places a simple upper limit on the heat transport by long-wavelength phonons and facilitates the comparison of the experimental data to recent numerical solutions of a Kubo formula using harmonic vibrations.

I. INTRODUCTION

In a disordered material, heat transport by lattice vibrations can be separated into two regimes. At low vibrational energies, the lattice vibrations are wavelike, i.e., phonons exist with well defined wave vector and velocity. In this regime, the kinetic formula is applicable: $\Lambda = Cvl/3$, where Λ is the thermal conductivity, C the heat capacity, v the velocity, and l the mean free path. As the energy E of the mode increases, the scattering rate increases as E^4 until $l^{-1} \sim k$ where k is the wave vector of the mode. Although the Boltzmann description is no longer valid in this high-energy regime, the magnitude of the thermal conductivity of disordered materials is in reasonable agreement with the kinetic formula with $l \simeq a$ (a=lattice constant), a fact first noted by Birch and Clark[1] and later by Kittel,[2] Slack,[3] and others.[4–6]

The experiments described below address this high-energy regime of heat transport by lattice vibrations in disordered materials. Analysis of thermal conductivity data has led to the proposal that a dominant fraction of the high-frequency modes are localized[7] and unable to contribute to heat transport unless anharmonic forces are present. Recently, numerical solution of a Kubo formula for an a-Si lattice with harmonic vibrations has concluded that the majority of the vibrational modes are not localized,[8–10] a conclusion supported by molecular dynamics calculations.[11,12] Calculations using the harmonic a-Si lattice show that velocity and wave vector are not well defined for the high-frequency modes and that heat transport takes place by coupling between nearly degenerate, extended vibrational modes, leading to a thermal conductivity comparable to $Cvl/3$ with $l \simeq a$. The purpose of our experiments on micrometer-thick a-Si:H films is to provide a quantitative test of the Kubo formula approach for calculating heat transport in disordered materials.

Figure 1 summarizes previously published data[13–18] on the thermal conductivity of a-Si and a-Si:H. The data show wide variations and it is not clear how much of the variation is intrinsic (due to film thickness and hydrogen content) or extrinsic (microstructure produced during deposition or experimental error). Data for other thin film materials also show wide scatter. Despite the importance of thermal properties of thin films to the performance of high-power laser optics,[19] optical storage disks,[20,21] and microelectronic circuits,[22,23] the thermal conductivity of thin film materials is poorly known.

Included in Fig. 1 are data for two 50-μm-thick a-Si:H films produced by plasma-assisted chemical vapor deposition (PACVD) and a 50-μm-thick film of a-Si prepared by sputtering.[16] These data were acquired using the 3ω method, a well tested measurement technique that was developed for measuring bulk materials[24] but is directly

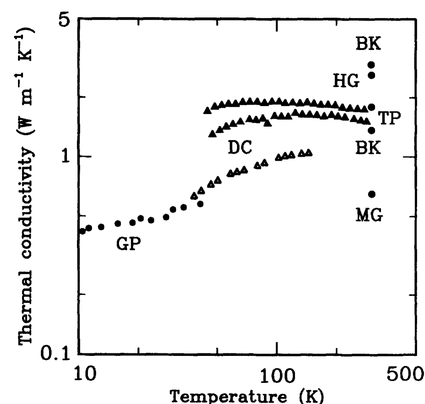

FIG. 1. Review of experimental data for the thermal conductivity of a-Si and a-Si:H. GP: 26-μm-thick sputtered a-Si measured parallel to the plane of the film, see Ref. 15; DC: 50-μm-thick plasma-assisted CVD a-Si:H (solid triangles) and sputtered a-Si (open triangles) measured with radial heat flow, see Ref. 16; BK: the effective thermal conductivity of two 1-μm-thick a-Si films, see Ref. 18; HG: 1.15-μm-thick a-Si, see Ref. 13; TP: 0.74-μm-thick evaporated a-Si, see Ref. 14; MG: 0.33-μm-thick a-Si prepared by ion implantation and annealing, see Ref. 17.

 ©1994 The American Physical Society

applicable to films greater than 30 μm thick. The cause of the higher value of the thermal conductivity of the PACVD a-Si:H relative to the sputtered, hydrogen-free film is puzzling. A systematic study of the dependence of the thermal conductivity on hydrogen content would clearly be desirable. Unfortunately, for most film deposition methods, the growth of films > 30 μm thick is extremely time consuming and as a result films that can be measured by the standard 3ω method are not readily available.

Motivated by these factors, we have developed an extension of the 3ω method for measurements of films 2000 Å to 5μm thick.[25] Films of this thickness can be routinely produced with nearly full density using magnetron sputtering. The use of data for thin films also facilitates our comparison of experiment and theory because the interface between film and substrate[26] places a simple upper limit on heat transport by long-wavelength phonons. Boundary scattering of phonons at the film/substrate interface limits the value of the mean free path to the film thickness. We can therefore eliminate the possibility of a large contribution to the thermal conductivity arising from a small minority of lattice modes with large mean free paths.

II. EXPERIMENTAL DETAILS

Our experimental technique for thin films is an extension of the 3ω method described previously.[24] A narrow metal line, prepared using thermal evaporation and photolithography serves as both the heater and the thermometer for the experiment. Our experiments use a 3000-Å layer of Au deposited on a 30-Å layer of Cr to enhance the adhesion of the Au metal line to the sample. The metal line is heated by Joule heating at frequency 2ω. The temperature oscillations of the metal line at frequency 2ω are measured through the small voltage oscillations at the third harmonic 3ω produced as a result of the temperature-dependent resistance of the metal line.[27,28] We use a digital signal processing lock-in amplifier[29] to produce the drive current and detect the third-harmonic voltage.

The geometry of the thin film measurement is shown in Fig. 2. We have chosen the dimensions so that the metal line is wide compared to the thickness of the film and therefore heat flow through the film is one dimensional. The temperature oscillations at the interface between film and substrate are identical to the standard 3ω method used for bulk samples. For a metal line of width $2b$ and length l the amplitude of the temperature oscillation at the substrate is given by[24]

$$\Delta T_s = \frac{P}{l\pi\Lambda}\int_0^\infty \frac{\sin^2(kb)}{(kb)^2(k^2+q^2)^{1/2}}\,dk\ , \quad q^2 = \left(\frac{2i\omega}{D}\right)\ , \tag{1}$$

where P is the power supplied to the line at frequency 2ω and D is the thermal diffusivity and Λ the thermal conductivity of the substrate. Equation (1) was derived with the assumption that heat enters the sample uniformly across the width of the metal line and that the metal line measures the average temperature of the surface without altering the heat flow. The agreement between Eq. (1) and experimental data for SiO_2 and MgO over a wide temperature range is excellent and can be improved further by using an effective value of b in Eq. (1) that is 10% larger than the actual value.

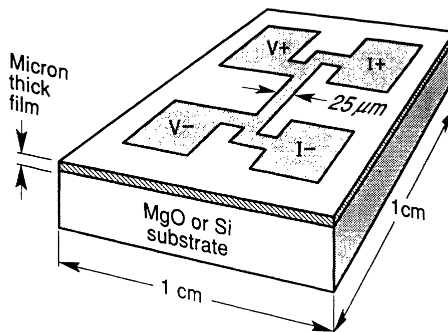

FIG. 2. Geometry for thin film thermal conductivity measurements using an extension of the 3ω method. The width of the metal line that serves as the heater and thermometer is typically 25 μm.

For our situation where the thermal conductivity of the film Λ_f is small compared to the thermal conductivity of the substrate, the thin film of thickness t behaves as a simple thermal resistance and adds a frequency-independent temperature oscillation to the result of Eq. (1):[30]

$$\Delta T_f = \frac{P}{l\Lambda_f}\frac{t}{2b}\ . \tag{2}$$

Figure 3 shows the raw experimental data for the metal line deposited directly on the (001) face of a MgO substrate and the data for the metal line deposited on a 0.5-μm-thick film of a-Si:H that was grown on MgO. For both sets of data, $2b = 25$ μm and $l = 3$ mm. The data for the MgO substrate have been scaled by the ratio of the power supplied to the metal lines in the two experiments. The data for the metal line deposited directly on MgO are in good agreement with Eq. (1) using $\Lambda = 51$ $\mathrm{W\,m^{-1}\,K^{-1}}$ [determined from the slope of the in-phase data versus $\ln(\omega)$] and a specific heat of 3.34 $\mathrm{J\,K^{-1}\,cm^{-3}}$.[31] As expected, the presence of the a-Si:H thin film produces a frequency-independent increase in the in-phase ΔT and no change in the out-of-phase signal.

Any new measurement method should be tested on a well characterized, standard material. Unfortunately, no thin film currently has a well known thermal conductivity. To evaluate the precision of our method, we chose to measure the thermal conductivity of a thermally grown a-SiO_2 layer on silicon based on the fact that the thermal conductivity near room temperature has been reported to be comparable to that of bulk a-SiO_2.[23,33] The oxidized wafer was purchased commercially and the details of the preparation are not available but a standard microelectronic process for thick oxides is oxidation of the silicon wafer at $\simeq 1100\,^\circ$C in an atmosphere containing

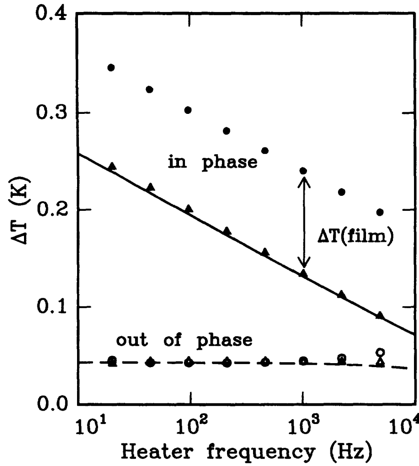

FIG. 3. Measured ΔT (rms) at T = 298 K for a MgO substrate (triangles) and for a 0.5-μm-thick a-Si:H film grown on a MgO substrate (circles). ΔT has been separated into the magnitude of the in-phase (filled symbols) and out-of-phase (open symbols) components. The solid and dashed lines are the calculated in-phase and out-of-phase contributions from the MgO substrate using Eq. (1). with an effective linewidth of 28-μm, 10% larger than the measured width of the metal line.

O_2 and H_2O vapor.[32] The thermal conductivity data are shown in Fig. 4. The data for the micrometer-thick film are in near perfect agreement with bulk SiO_2 over the entire temperature range of our measurement, 80–400 K.

The fact that the data for a micrometer-thick film of a-SiO_2 are nearly identical to those for bulk a-SiO_2 gives further support to the assertion that long-wavelength phonons do not make a significant contribution to heat transport[34,35] near room temperature in a-SiO_2. If long-wavelength phonons with $l > 1$ μm contributed to heat transport in bulk a-SiO_2, then the conductivity of the thin film would have been reduced by scattering at the film/substrate interface.

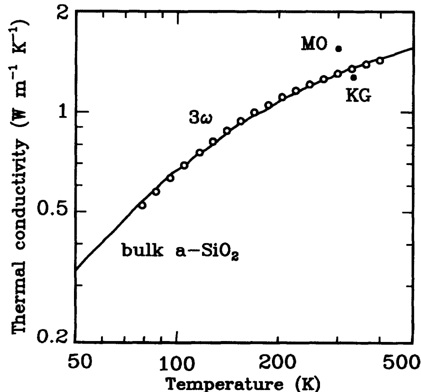

FIG. 4. Data (open circles) for a 0.99-μm-thick a-SiO_2 layer thermally grown on Si(001). Data for bulk a-SiO_2 are shown as the solid line, see Ref. 24. Two data points at room temperature marked "MO" and "KG" are also for thermally grown oxide films, see Refs. 33 and 23.

We deposited a-Si:H thin films on crystalline Si and MgO substrates by dc reactive magnetron sputtering of a silicon target in an Ar-H_2 atmosphere.[36,37] MgO substrates were used for low hydrogen content films (1.0 and 7.5 % H_2) because these films did not adequately insulate the metal line from the electrical effects of Si substrates. The Ar partial pressure was fixed at 1.5 mTorr. Hydrogen content was varied by changing the H_2 partial pressure and substrate temperature. Hydrogen content of the films was determined from infrared absorption of Si-H vibrational modes as described by Langford *et al.*[38] The microstructure of films prepared in our growth chambers has been characterized using small-angle x-ray scattering and spectroscopic ellipsometry.[39,40] The void fraction of films grown under similar conditions is 3–5 %. We measure the a-Si:H film thickness using interference fringes observed in infrared transmission.

Metal films for the heater/thermometer line are then deposited on the a-Si:H samples using thermal evaporation. In order to ensure that the hydrogen content and crystallinity of the a-Si:H samples are not altered by the metal deposition, we attach the samples to a large copper plate to maintain the temperature of the samples near room temperature and therefore far below the substrate temperature during deposition of the a-Si:H samples. We have not characterized the composition or structure of the interface between the metal line and the a-Si:H film but we expect that the 30-Å Cr adhesion layer will react with a-Si:H and its native oxide to form a disordered silicide-oxide layer $\sim$ 30 Å thick. This interfacial layer is too thin to significantly affect our thermal conductivity data.

III. RESULTS AND DISCUSSION

Five samples of a-Si:H were measured in this study; Table I lists the film thickness, hydrogen content, and substrate temperature for each. While the highest-conductivity film does have the lowest hydrogen content, we do not observe a systematic change in the conductivity with hydrogen content (see Fig. 5). For example, near room temperature the conductivity of the 15% film is $\sim$ 10% larger than that of the 7.5 % film, despite having similar film thickness (1.45 versus 1.0 μm). Small variation in film density between different films is a pos-

TABLE I. a-Si:H film composition, thickness, and substrate temperature during deposition.

Hydrogen content (at. %)	Film thickness (μm)	Substrate temperature (°C)	Substrate
1	0.52	230	MgO
7.5	1.02	230	MgO
15	1.45	260	Si
16	1.65	275	Si
20	0.22	230	Si

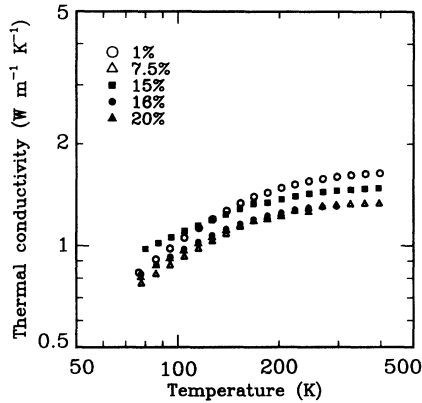

FIG. 5. Thermal conductivity of a-Si:H. The key to each symbol gives the hydrogen content in atomic percent. Substrate temperature and film thickness are listed in Table I.

sible cause of the spread in our data.

Since the thermal conductivity of these films has only a weak dependence on hydrogen content, we can rule out hydrogen composition as a cause of the variation in the data reviewed in Fig. 1. Near room temperature, the data shown in Fig. 5 agree reasonably well with the data for the 50-μm-thick a-Si:H samples prepared by plasma-assisted chemical vapor deposition (PACVD). Below 100 K, the thermal conductivity of micrometer-thick a-Si:H is smaller than the PACVD thick films because of scattering of long-wavelength phonons at the interface between the film and substrate.

In Ref. 10, contributions to the thermal conductivity from modes with energy < 10 meV cannot be calculated using the Kubo formula because of the finite size of the computational unit cell. Since the thermal conductivity of an infinite, harmonic solid is infinite at all temperatures, Feldman and co-workers[10] invoked scattering of phonons by the tunneling states to produce a finite mean free path for low-frequency phonons. This procedure requires an extrapolation of the scattering rates derived at $T < 10$ K to room temperature. While the extrapolation is plausible, few experimental data are available to check the validity of the procedure.

Our experimental system, a micrometer-thick film, provides a straightforward limit to the mean free path of the propagating vibrational modes. Phonon scattering at the interface between the film and substrate limits the mean free path to the film thickness. Therefore the thermal conductivity of our *finite* size specimen does not diverge even if the lattice is assumed to be perfectly harmonic.

We calculate the contribution to heat transport from modes with energy < 10 meV by including boundary scattering at the film/substrate interface and the strength of Rayleigh scattering determined by the calculation of Ref. 10. A Debye model is used that treats separately the transverse and longitudinal acoustic modes. A fit to the mode diffusivity as a function of energy from Fig. 1 of Ref. 10 gives $D(E) = B_0/E^4$, $B_0 = 230$ cm^2 sec^{-1} meV^4. This mode diffusivity is the average of the diffusivity of transverse and longitudinal modes weighted by the respective density of states. We use values for the transverse and longitudinal speeds of sound suggested by the low-temperature specific heat[41] and scaling from values for crystalline Si: $v_t = 4.37$ km sec^{-1}, $v_l = 7.36$ km sec^{-1}. We also assume that the strength of the Rayleigh scattering for transverse and longitudinal modes is given by $\Gamma = A_0\nu^4$ where A_0 is a constant independent of mode,[42] Γ is the scattering rate, and ν the vibrational frequency of the mode. Our fit to $D(E)$ gives $A_0 = 2.9 \times 10^{-37}$ sec^3. Including a boundary scattering term at 0.5-μm gives a thermal conductivity of 0.31 W m^{-1} K^{-1} at $T > 50$ K for modes with $E < 10$ meV. This value is only weakly dependent on the film thickness, varying as $\sim t^{0.25}$ but more strongly dependent on the size of A_0; we find that a change in A_0 of a factor of 3 produces a factor of 2 change in the calculated contribution to the thermal conductivity from low-frequency modes.

Figure 6 displays the data for the 1.0% H_2 film (highest curve in Fig. 5) along with the thermal conductivity calculated from Ref. 10. The dashed line shows the calculated thermal conductivity increased by 0.31 W m^{-1} K^{-1} as described above to account for heat transport by propagating modes with $E < 10$ meV. The discrepancy is $< 15\%$ over the entire temperature range of our data, 80–400 K.

While we expect that the thermal conductivity is relatively insensitive to the details of the atomic structure, we believe the comparison between theory and experiment shown in Fig. 6 strongly supports the description of heat transport in disordered materials developed in Ref. 10, namely, that the dominant heat transport mechanism is coupling between nearly degenerate, extended, but nonpropagating vibrational modes.

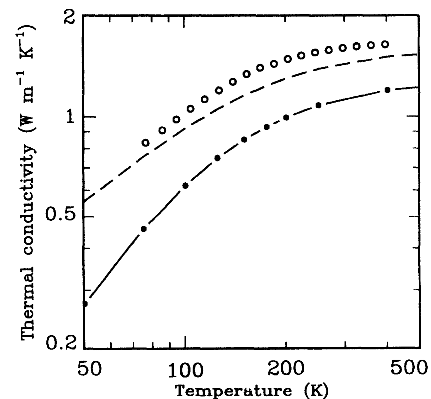

FIG. 6. Comparison of theoretical results of Ref. 10 (filled circles with solid connecting line) with data for a-Si:H with 1 at. % hydrogen (open circles). The dashed line shows our modification of the results of Ref. 10 to include contributions to the thermal conductivity from vibrational modes with energies less than 10 meV (dashed line) using a Debye model with no free parameters. The strength of Rayleigh scattering is determined by a fit to the theoretically determined mode diffusivity and boundary scattering at the film/substrate interfaces limits the phonon mean free path to the film thickness.

ACKNOWLEDGMENTS

This work was supported by the U.S. Department of Energy grant DEFG02-91-ER45439 through the University of Illinois Materials Research Laboratory and the exploratory research program of the Electric Power Research Institute (EPRI RP 8001-7). Film thickness measurements were carried out in the Center for Microanalysis of Materials, University of Illinois, which is supported by the U.S. Department of Energy under grant DEFG02-91-ER45439. We also thank Joe Feldman for transmitting the results of his study and several helpful discussions.

---

[1] F. Birch and H. Clark, Am. J. Sci. **238**, 529 (1940).
[2] C. Kittel, Phys. Rev. **75**, 972 (1948).
[3] G. A. Slack, in *Solid State Physics: Advances in Research and Applications*, edited by F. Seitz and A. G. Turnball (Academic Press, New York, 1979), Vol. 34, p. 1; see, in particular, p. 57.
[4] J. E. Graebner, B. Golding, and L. C. Allen, Phys. Rev. B **34**, 5696 (1986).
[5] David G. Cahill and R. O. Pohl, Annu. Rev. Phys. Chem. **39**, 93 (1988).
[6] David G. Cahill, S. K. Watson, and R. O. Pohl, Phys. Rev. B **46**, 6131 (1992).
[7] R. Orbach, Philos. Mag. B **65**, 289 (1992).
[8] Philip B. Allen and Joseph L. Feldman, Phys. Rev. Lett. **62**, 645 (1989).
[9] Philip B. Allen and Joseph L. Feldman, Phys. Rev. B **48**, 12 581 (1993).
[10] Joseph L. Feldman, Mark D. Kuge, Philip B. Allen, and Frederick Wooten, Phys. Rev. B **48**, 12 589 (1993).
[11] P. Sheng and M. Y. Zhou, Science **253**, 539 (1991).
[12] Y. H. Lee, R. Biswas, C. M. Soukoulis, C. Z. Wang, C. T. Chan, and K. M. Ho, Phys. Rev. B **43**, 6573 (1991).
[13] H. J. Goldsmid, M. M. Kaila, and G. L. Paul, Phys. Status Solidi A **76**, K31 (1983).
[14] T. Papa, F. Scudieri, M. Marinelli, U. Zammit, and G. Cembali, J. Phys. (Paris) Coll. **44**, C5-73 (1983).
[15] G. Pompe and E. Hegenbarth, Phys. Status Solidi B **147**, 103 (1988).
[16] David G. Cahill, Henry E. Fischer, Tom Klitsner, E. T. Swartz, and R. O. Pohl, J. Vac. Sci. Technol. A **7**, 1259 (1989).
[17] M. G. Grimaldi, P. Baeri, and M. A. Malvezzi, Phys. Rev. B **44**, 1546 (1991).
[18] B. S. W. Kuo, J. C. M. Li, and A. W. Schmid, Appl. Phys. A **55**, 289 (1992).
[19] Arthur H. Guenther and John K. McIver, Thin Solid Films **163**, 203 (1988).
[20] D. Raasch and S. Klahn, J. Magn. Magn. Mater. **93**, 365 (1991).
[21] Mark D. Schultz, Joshua M. Freedman, Robert S. Weng, and Mark K. Kryder, J. Appl. Phys. **69**, 4948 (1991).
[22] Harry A. Schafft, John S. Suehle, and Paul G. A. Mirel, IEEE Proc. Microelectron. Test Struct. **2**, 121 (1989).
[23] K. E. Goodson, M. I. Flik, L. T. Su, and Dimitri A. Antoniadis, IEEE Electron Device Lett. **14**, 490 (1993).
[24] David G. Cahill, Rev. Sci. Instrum. **61**, 802 (1990).
[25] David G. Cahill (unpublished).
[26] E. T. Swartz and R. O. Pohl, Appl. Phys. Lett. **51**, 2200 (1987).
[27] N. O. Birge and S. R. Nagel, Phys. Rev. Lett. **54**, 2674 (1985).
[28] N. O. Birge and S. R. Nagel, Rev. Sci. Instrum. **58**, 1464 (1987).
[29] Stanford Research Systems, Sunnyvale, CA.
[30] The edge effects in our geometry are identical to the effects of fringing fields on the capacitance of a strip line conductor and can be corrected for by using an effective linewidth of $2b + 0.88t$, where $2b$ is the actual linewidth and t the film thickness. See H. A. Wheeler, IEEE Trans. Microwave Theory Tech. **13**, 172 (1965).
[31] *Thermophysical Properties of Matter,* edited by Y. S. Touloukian (IFI/Plenum, New York, 1970).
[32] *Electronic Materials Science and Technology,* edited by Shyam P. Murarka and Martin C. Peckerar (Academic Press, San Diego, CA, 1989); see p. 112.
[33] M. Okuda and S. Ohkubo, Thin Solid Films **213**, 176 (1992).
[34] M. S. Love and A. C. Anderson, Phys. Rev. B **42**, 1845 (1990).
[35] David G. Cahill, R. B. Stephens, R. H. Tait, Susan K. Watson, and R. O. Pohl, in *Thermal Conductivity 21*, edited by C. J. Cremers and H. A. Fine (Plenum Press, New York, 1990), pp. 3–16.
[36] M. Pinarbasi, N. Maley, A. Myers, and J. R. Abelson, Thin Solid Films **171**, 217 (1989).
[37] G. F. Feng, M. Katiyar, N. Maley, and J. R. Abelson, Appl. Phys. Lett. **59**, 330 (1991).
[38] A. A. Langford, M. L. Fleet, B. P. Nelson, W. A. Lanford, and N. Maley, Phys. Rev. B **45**, 13 367 (1992).
[39] Y. Chen, S. J. Jones, D. L. Williamson, S. Yang, N. Maley, and J. R. Abelson, in *Amorphous Silicon Technology-1992*, edited by M. J. Thompson *et al.*, MRS Symposia Proceedings No. 258 (Materials Research Society, Pittsburgh, 1992), p. 311.
[40] G. F. Feng, M. Katiyer, J. R. Abelson, and N. Maley, J. Non-Cryst. Solids, **137&138**, 331 (1991).
[41] M. Mertig, G. Pompe, and E. Hegenbarth, Solid State Commun. **49**, 369 (1984).
[42] S. Tamura, J. A. Shields, J. A. Shields, M. T. Ramsbey, and J. P. Wolfe, in *Phonon Scattering in Condensed Matter VII*, edited by M. Meissner and R. O. Pohl (Springer Verlag, Berlin, 1993), p. 79; P. G. Klemens, Proc. Phys. Soc. London, Sect. A **68**, 1113 (1955).

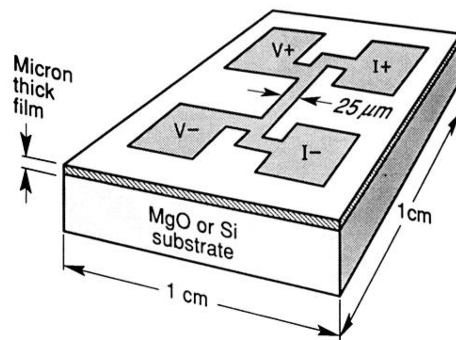

FIG. 2. Geometry for thin film thermal conductivity measurements using an extension of the 3ω method. The width of the metal line that serves as the heater and thermometer is typically 25 μm.